Eur. Phys. J. C 25, 575–581 (2002)
Digital Object Identifier (DOI) 10.1007/s10052-002-1008-9

THE EUROPEAN PHYSICAL JOURNAL C

The exclusive $B_s \to \phi\ell^+\ell^-$ decay in the two Higgs doublet models

G. Erkol[a], G. Turan[b]

Middle East Technical University Physics Dept. Inonu Bul., 06531 Ankara, Turkey

Received: 27 March 2002 / Revised version: 3 July 2002 /
Published online: 20 September 2002 – © Springer-Verlag / Società Italiana di Fisica 2002

Abstract. We study the differential branching ratio, the branching ratio and the forward–backward asymmetry for exclusive $B_s \to \phi\ell^+\ell^-$ decay in the two Higgs doublet model. We analyze the dependences of these quantities on the model parameters and show that these observables are highly sensitive to new physics and hence may provide a powerful probe of the SM and beyond.

1 Introduction

The analysis of flavor-changing neutral current (FCNC) decays is one of the most promising research areas in particle physics from both the theoretical and the experimental side. The rare B-meson decays induced by the FCNC $b \to s$ transition have received special attention since their investigation opens up the possibility of a more precise determination of the fundamental parameters of the standard model (SM), such as the elements of the Cabibbo–Kobayashi–Maskawa (CKM) matrix, the leptonic decay constants etc. In addition, the studies on the rare B-meson decays open a window to investigate the physics beyond the SM, such as the two Higgs doublet model (2HDM), the minimal supersymmetric extension of the SM (MSSM) [1], etc.; to test these models and make estimates about their free parameters.

The difficulties present in the experimental investigation of the inclusive decays stimulate the study of exclusive decays. There exist now upper limits on the branching ratios of $B^0 \to K^{0*}\mu^+\mu^-$ and $B^+ \to K^+\mu^+\mu^-$, given by the CDF collaboration [2]:

$$\mathrm{BR}(B^0 \to K^{0*}\mu^+\mu^-) < 4.0 \times 10^{-6},$$
$$\mathrm{BR}(B^+ \to K^+\mu^+\mu^-) < 5.2 \times 10^{-6}.$$

With these measured upper limits and also the recent measurement of the branching ratio of $B \to K\ell^+\ell^-$ with $\ell = e, \mu$,

$$\mathrm{BR}(B \to K\ell^+\ell^-) = (0.75^{+0.25}_{-0.21} \pm 0.09) \times 10^{-6}$$

at KEK [3], the processes $B \to (K, K^*)\ell^+\ell^-$ have received great interest so that their theoretical calculation has been the subject of many investigations in the SM and beyond [4–18]. Along this line, the exclusive decays induced by the $b \to s\ell^+\ell^-$ transition, like $B_s \to \phi\ell^+\ell^-$, become also attractive since the SM predicts a relatively larger branching ratio, which is measurable in the near future. On the other hand, the theoretical analysis of exclusive decays is more complicated and contains substantial uncertainties due to the hadronic form factors, which need non-perturbative methods for their calculations. One of the methods that can be used to calculate the hadronic matrix elements is the three parameter fit of the light-cone QCD sum rule. In [19], the form factors for $b \to s\ell^+\ell^-$ induced exclusive $B_s \to \phi\ell^+\ell^-$ decay have been calculated in the framework of this method. More recently, this process has also been investigated in a different context, namely using a so-called constituent quark–meson model (CQM) based on quark–meson interactions [20].

In this paper we investigate the exclusive $B_s \to \phi\ell^+\ell^-$ decay in the framework of the 2HDM. The transitions where B-meson decays into a vector meson, like K^* [4–18] and ρ [21–26], have been extensively studied in the literature both in the SM and beyond. We calculate the dependence of the branching ratio (BR) and the forward–backward asymmetry (A_{FB}) of the exclusive $B_s \to \phi\ell^+\ell^-$ decay on the model parameters in the model I, II and III versions of the 2HDM and show that for some values of these parameters especially model III gives significant contributions to the BR and A_{FB}.

This paper is organized as follows: In Sect. 2, after we present the theoretical framework of the 2HDMs and the leading order QCD corrected effective Hamiltonian for the process $b \to s\ell^+\ell^-$, we calculate the differential BR and the A_{FB} of the exclusive $B_s \to \phi\ell^+\ell^-$ decay. Section 3 is devoted to the numerical analysis and the discussions.

2 The theoretical framework

Before presenting the details of our calculations, we would like to summarize the main essential points of the 2HDM,

[a] e-mail: gurerk@newton.physics.metu.edu.tr
[b] e-mail: gsevgur@metu.edu.tr

which is one of the most popular extensions of the SM. The 2HDM has two complex Higgs doublets instead of only one in the SM. In general, the 2HDM possesses tree-level FCNCs that can be avoided by imposing an ad hoc discrete symmetry [27]. As a result, there appear two different choices, namely model I and II, depending on whether up-type and down-type quarks couple to the same or two different Higgs doublets, respectively. Model II has been more attractive since its Higgs sector is the same as the Higgs sector in the supersymmetric models. The physical content of the Higgs sector includes three neutral Higgs bosons, H^0, h^0 and A^0, and a pair of charged Higgs bosons $H^\pm$. In these models the interaction vertices of the Higgs bosons and fermions depend on the ratio $\tan\beta = v_1/v_2$, where v_1 and v_2 are the vacuum expectation values of the first and the second Higgs doublet respectively, and it is a free parameter in the model. The constraints on $\tan\beta$ are usually obtained from B–$\bar{B}$, K–$\bar{K}$ mixing, the $b \to s\gamma$ decay width and semileptonic decay $b \to c\tau\bar{\nu}$ and is given by [28]

$$0.7 \leq \tan\beta \leq 0.52 \left(\frac{m_{H^\pm}}{1\,\mathrm{GeV}}\right), \tag{1}$$

and the lower bound $m_{H^\pm} \geq 200$ GeV has also been given in [28].

In a more general 2HDM, namely model III [29,30], no discrete symmetry is imposed and there appear FCNC naturally at the tree level. We note that in model III, FCNC receiving contributions from the first two generations are highly suppressed, which is confirmed by low energy experiments. As for those involving the third generation, it is possible to impose some restrictions on them with the existing experimental results. Since the popular models I and II are special cases of the more general model III, we will give here the details of model III only.

The Yukawa Lagrangian in this general case is written

$$\begin{aligned}\mathcal{L}_\mathrm{Y} = {} & \eta^U_{ij}\bar{Q}_{i\mathrm{L}}\tilde{\psi}_1 U_{j\mathrm{R}} + \eta^D_{ij}\bar{Q}_{i\mathrm{L}}\psi_1 D_{j\mathrm{R}} + \xi^{U\dagger}_{ij}\bar{Q}_{i\mathrm{L}}\tilde{\psi}_2 U_{j\mathrm{R}} \\ & + \xi^D_{ij}\bar{Q}_{i\mathrm{L}}\psi_2 D_{j\mathrm{R}} + \mathrm{h.c.},\end{aligned} \tag{2}$$

where i, j are family indices of quarks, L and R denote chiral projections $1/2(1 \mp \gamma_5)$, ψ_m for $m = 1, 2$, are the two scalar doublets, $Q_{i\mathrm{L}}$ are quark doublets, $U_{j\mathrm{R}}$, $D_{j\mathrm{R}}$ are the corresponding quark singlets, $\eta^{U,D}_{ij}$ and $\xi^{U,D}_{ij}$ are the matrices of the Yukawa couplings. We can choose two scalar doublets φ_1 and φ_2 in the following form:

$$\begin{aligned}\varphi_1 &= \frac{1}{\sqrt{2}}\left[\begin{pmatrix}0\\ v+H^0\end{pmatrix} + \begin{pmatrix}\sqrt{2}\chi^+\\ \mathrm{i}\chi^0\end{pmatrix}\right]; \\ \varphi_2 &= \frac{1}{\sqrt{2}}\begin{pmatrix}\sqrt{2}H^+\\ H_1 + \mathrm{i}H_2\end{pmatrix},\end{aligned} \tag{3}$$

with the vacuum expectation values,

$$\langle\varphi_1\rangle = \frac{1}{\sqrt{2}}\begin{pmatrix}0\\ v\end{pmatrix}; \quad \langle\varphi_2\rangle = 0, \tag{4}$$

so that the first doublet ψ_1 is the same as the one in the SM, while the second doublet contains all the new particles. Further, we take H_1 and H_2 as the mass eigenstates h^0 and A^0, respectively.

After the rotation that diagonalizes the quark mass eigenstates, the part of the Lagrangian that is responsible for the FCNC at the tree level looks like

$$\mathcal{L}_{\mathrm{Y,FC}} = -H^\dagger\bar{\mathcal{U}}[V_\mathrm{CKM}\xi^D_N R - \xi^{U\dagger}_N V_\mathrm{CKM} L]\mathcal{D}, \tag{5}$$

where $\mathcal{U}(\mathcal{D})$ represents the mass eigenstates of up- (down-) type quarks. In this work, we adopt the following redefinition of the Yukawa couplings:

$$\xi^{U,D}_N = \sqrt{\frac{4G_\mathrm{F}}{\sqrt{2}}}\bar{\xi}^{U,D}_{N,ij}. \tag{6}$$

The next step is to calculate the matrix elements for the inclusive $b \to s\ell^+\ell^-$ decay in model III including the QCD corrections. For this, the effective Hamiltonian method provides a powerful framework. The procedure is to match the full theory with the effective theory, which is obtained by integrating out the heavy degrees of freedom, i.e., t quark, $W^\pm$, $H^\pm$, h^0 and H^0 in our case, at the high scale of $\mu = m_W$, and then calculate the Wilson coefficients at the lower scale $\mu \sim \mathcal{O}(m_b)$ using the renormalization group equations. Following these steps, one can obtain the effective Hamiltonian governing the $b \to s\ell^+\ell^-$ transitions, in model III in terms of a set of operators

$$\mathcal{H}_\mathrm{eff} = \frac{4G_\mathrm{F}}{\sqrt{2}}V_{tb}V^*_{ts}\left\{\sum_{i=1}^{10} C_i(\mu)O_i(\mu)\right\}. \tag{7}$$

Here, O_1 and O_2 are the *current–current operators*, $O_3, \ldots,$ O_6 are usually named the *QCD penguin operators*, O_7 and O_8 are the *magnetic penguin operators* and O_9 and O_{10} are the *semileptonic electroweak penguin operators*. $C_i(\mu)$ are Wilson coefficients renormalized at the scale μ. The operator basis in the 2HDM for our process can be found in [31,32].

Denoting the Wilson coefficients for the relevant process in the SM with $C^\mathrm{SM}_i(m_W)$ and the additional charged Higgs contributions with $C^H_i(m_W)$, we have the initial values given by [31,33]

$$\begin{aligned}C^\mathrm{SM}_{1,3,\ldots 6}(m_W) &= 0, \\ C^\mathrm{SM}_2(m_W) &= 1, \\ C^\mathrm{SM}_7(m_W) &= \frac{3x_t^3 - 2x_t^2}{4(x_t-1)^4}\ln x_t + \frac{-8x_t^3 - 5x_t^2 + 7x_t}{24(x_t-1)^3}, \\ C^\mathrm{SM}_8(m_W) &= -\frac{3x_t^2}{4(x_t-1)^4}\ln x_t + \frac{-x_t^3 + 5x_t^2 + 2x_t}{8(x_t-1)^3}, \\ C^\mathrm{SM}_9(m_W) &= -\frac{1}{\sin^2\theta_\mathrm{W}}B(x_t) \\ &\quad + \frac{1 - 4\sin^2\theta_\mathrm{W}}{\sin^2\theta_\mathrm{W}}C(x_t) - D(x_t) + \frac{4}{9}, \\ C^\mathrm{SM}_{10}(m_W) &= \frac{1}{\sin^2\theta_\mathrm{W}}(B(x_t) - C(x_t)),\end{aligned}$$

and

$$\begin{aligned} C^H_{1,\ldots,6}(m_W) &= 0, \\ C^H_7(m_W) &= Y^2 F_1(y_t) + XY F_2(y_t), \\ C^H_8(m_W) &= Y^2 G_1(y_t) + XY G_2(y_t), \\ C^H_9(m_W) &= Y^2 H_1(y_t), \\ C^H_{10}(m_W) &= Y^2 L_1(y_t), \end{aligned} \tag{8}$$

where

$$\begin{aligned} x_t &= \frac{m_t^2}{m_W^2}, \quad y_t = \frac{m_t^2}{m_{H^\pm}^2}, \\ X &= \frac{1}{m_b}\left(\bar{\xi}^D_{N,bb} + \bar{\xi}^D_{N,db}\frac{V_{td}}{V_{tb}}\right), \\ Y &= \frac{1}{m_t}\left(\bar{\xi}^U_{N,tt} + \bar{\xi}^U_{N,tc}\frac{V^*_{cd}}{V^*_{td}}\right). \end{aligned} \tag{9}$$

Note that the results for model I and II can be obtained from model III by the following substitutions:

$$\begin{aligned} &Y \to \cot\beta, \quad XY \to -\cot^2\beta \quad \text{for model I}, \\ &Y \to \cot\beta, \quad XY \to 1 \quad \text{for model II}. \end{aligned}$$

The explicit forms of the functions $F_{1(2)}(y_t)$, $G_{1(2)}(y_t)$, $H_1(y_t)$ and $L_1(y_t)$ in (8) are given by

$$\begin{aligned} F_1(y_t) &= \frac{y_t(7-5y_t-8y_t^2)}{72(y_t-1)^3} + \frac{y_t^2(3y_t-2)}{12(y_t-1)^4}\ln y_t, \\ F_2(y_t) &= \frac{y_t(5y_t-3)}{12(y_t-1)^2} + \frac{y_t(-3y_t+2)}{6(y_t-1)^3}\ln y_t, \\ G_1(y_t) &= \frac{y_t(-y_t^2+5y_t+2)}{24(y_t-1)^3} + \frac{-y_t^2}{4(y_t-1)^4}\ln y_t, \\ G_2(y_t) &= \frac{y_t(y_t-3)}{4(y_t-1)^2} + \frac{y_t}{2(y_t-1)^3}\ln y_t, \\ H_1(y_t) &= \frac{1-4\sin^2\theta_{\rm W}}{\sin^2\theta_{\rm W}}\frac{xy_t}{8}\left[\frac{1}{y_t-1} - \frac{1}{(y_t-1)^2}\ln y_t\right] \\ &\quad - y_t\left[\frac{47y_t^2-79y_t+38}{108(y_t-1)^3} - \frac{3y_t^3-6y_t+4}{18(y_t-1)^4}\ln y_t\right], \\ L_1(y_t) &= \frac{1}{\sin^2\theta_{\rm W}}\frac{xy_t}{8}\left[-\frac{1}{y_t-1} + \frac{1}{(y_t-1)^2}\ln y_t\right]. \end{aligned} \tag{10}$$

Finally, the initial values of the coefficients in model III are

$$C_i^{\rm 2HDM}(m_W) = C_i^{\rm SM}(m_W) + C_i^H(m_W). \tag{11}$$

Using these initial values, we can calculate the coefficients $C_i^{\rm 2HDM}(\mu)$ at any lower scale in the effective theory with five quarks, namely u, c, d, s, b, similar to the SM case [31–34].

The Wilson coefficients playing the essential role in this process are $C_7^{\rm 2HDM}(\mu)$, $C_9^{\rm 2HDM}(\mu)$, $C_{10}^{\rm 2HDM}(\mu)$. For completeness, we also give their explicit expressions:

$$C_7^{\rm eff}(\mu) = C_7^{\rm 2HDM}(\mu) + Q_d(C_5^{\rm 2HDM}(\mu) + N_c C_6^{\rm 2HDM}(\mu)),$$

where the leading order QCD corrected Wilson coefficient $C_7^{\rm LO,2HDM}(\mu)$ is given by [34,31,32]

$$\begin{aligned} C_7^{\rm LO,2HDM}(\mu) &= \eta^{16/23} C_7^{\rm 2HDM}(m_W) \\ &\quad + (8/3)(\eta^{14/23} - \eta^{16/23}) C_8^{\rm 2HDM}(m_W) \\ &\quad + C_2^{\rm 2HDM}(m_W)\sum_{i=1}^{8} h_i \eta^{a_i}, \end{aligned} \tag{12}$$

and $\eta = \alpha_{\rm s}(m_W)/\alpha_{\rm s}(\mu)$, h_i and a_i are the numbers which appear during the evaluation [34].

$C_9^{\rm eff}(\mu)$ contains a perturbative part and a part coming from LD effects due to conversion of the real $\bar{c}c$ into a lepton pair $\ell^+\ell^-$:

$$C_9^{\rm eff}(\mu) = C_9^{\rm pert}(\mu) + Y_{\rm reson}(s), \tag{13}$$

where

$$\begin{aligned} C_9^{\rm pert}(\mu) &= C_9^{\rm 2HDM}(\mu) \\ &\quad + h(z,s)[3C_1(\mu) + C_2(\mu) + 3C_3(\mu) + C_4(\mu) \\ &\quad + 3C_5(\mu) + C_6(\mu)] \\ &\quad - \frac{1}{2}h(1,s)\,(4C_3(\mu) + 4C_4(\mu) + 3C_5(\mu) + C_6(\mu)) \\ &\quad - \frac{1}{2}h(0,s)\,[C_3(\mu) + 3C_4(\mu)] \\ &\quad + \frac{2}{9}\,(3C_3(\mu) + C_4(\mu) + 3C_5(\mu) + C_6(\mu))\,, \end{aligned} \tag{14}$$

and $z = m_c/m_b$. The functions $h(z,s)$ arise from the one loop contributions of the four quark operators O_1,...,O_6 and their explicit forms can be found in [32,34]

It is possible to parameterize the resonance $\bar{c}c$ contribution $Y_{\rm reson}(s)$ in (13) using a Breit–Wigner shape with normalizations fixed by data which is given by [35]

$$\begin{aligned} Y_{\rm reson}(s) &= -\frac{3}{\alpha_{\rm em}^2}\kappa \sum_{V_i=\psi_i} \frac{\pi\Gamma(V_i \to \ell^+\ell^-)m_{V_i}}{q^2 - m_{V_i} + {\rm i}m_{V_i}\Gamma_{V_i}} \\ &\quad \times \Big[(3C_1(\mu) + C_2(\mu) + 3C_3(\mu) + C_4(\mu) \\ &\quad + 3C_5(\mu) + C_6(\mu))\Big]. \end{aligned} \tag{15}$$

The phenomenological parameter κ in (15) is taken as 2.3 so as to reproduce the correct value of the branching ratio ${\rm BR}(B \to J/\psi X \to X\ell\bar{\ell}) = {\rm BR}(B \to J/\psi X){\rm BR}(J/\psi \to X\ell\bar{\ell})$.

Neglecting the mass of the s quark, the effective short distance Hamiltonian for the $b \to s\ell^+\ell^-$ decay leads to the QCD corrected matrix element:

$$\begin{aligned} \mathcal{M} &= \frac{G_{\rm F}\alpha}{2\sqrt{2}\pi}V_{tb}V_{ts}^*\Big\{C_9^{\rm eff}(m_b)\bar{s}\gamma_\mu(1-\gamma_5)b\bar{\ell}\gamma^\mu\ell \\ &\quad + C_{10}(m_b)\bar{s}\gamma_\mu(1-\gamma_5)b\bar{\ell}\gamma^\mu\gamma_5\ell \\ &\quad - 2C_7^{\rm eff}(m_b)\frac{m_b}{q^2}\bar{s}{\rm i}\sigma_{\mu\nu}q^\nu(1+\gamma_5)b\bar{\ell}\gamma^\mu\ell\Big\}, \end{aligned} \tag{16}$$

where q is the momentum transfer.

2.1 The exclusive $B_s \to \phi\ell^+\ell^-$ decay in the 2HDM

In this section we calculate the BR and the $A_{\rm FB}$ of the $B_s \to \phi\ell^+\ell^-$ decay. In order to find these physically measurable quantities at the hadronic level, we need the following matrix elements: $\langle\phi(p_\phi,\varepsilon)|\bar{s}\gamma_\mu(1-\gamma_5)b|B(p_B)\rangle$ and $\langle\phi(p_\phi,\varepsilon)|\bar{s}\mathrm{i}\sigma_{\mu\nu}q^\nu(1+\gamma_5)b|B(p_B)\rangle$, which can be parameterized in terms of form factors. Using the parameterization of the form factors as in [12], we get the following expression for the matrix element of the $B_s \to \phi\ell^+\ell^-$ decay:

$$\begin{aligned}\mathcal{M}^{B\to\phi} = \frac{G_{\rm F}\alpha}{2\sqrt{2}\pi}V_{tb}V_{ts}^*\Big\{&\bar{\ell}\gamma_\mu\ell\Big[2A\epsilon_{\mu\nu\lambda\sigma}\varepsilon^{*\nu}p_\phi^\lambda p_B^\sigma + \mathrm{i}B\varepsilon_\mu^* \\ &- \mathrm{i}C(p_B+p_\phi)_\mu(\varepsilon^* q) - \mathrm{i}D(\varepsilon^* q)q_\mu\Big] \\ &+ \bar{\ell}\gamma_\mu\gamma_5\ell\Big[2E\epsilon_{\mu\nu\lambda\sigma}\varepsilon^{*\nu}p_\phi^\lambda p_B^\sigma + \mathrm{i}F\varepsilon_\mu^* \\ &- \mathrm{i}G(\varepsilon^* q)(p_B+p_\phi) - \mathrm{i}H(\varepsilon^* q)q_\mu\Big]\Big\},\end{aligned} \tag{17}$$

where

$$\begin{aligned}A &= C_9^{\rm eff}\frac{V}{m_B+m_\phi} + 4\frac{m_b}{q^2}C_7^{\rm eff}T_1, \\ B &= (m_B+m_\phi)\left(C_9^{\rm eff}A_1 + \frac{4m_b}{q^2}(m_B-m_\phi)C_7^{\rm eff}T_2\right), \\ C &= C_9^{\rm eff}\frac{A_2}{m_B+m_\phi} + 4\frac{m_b}{q^2}C_7^{\rm eff}\left(T_2 + \frac{q^2}{m_B^2-m_\phi^2}T_3\right), \\ D &= 2C_9^{\rm eff}\frac{m_\phi}{q^2}(A_3-A_0) - 4C_7^{\rm eff}\frac{m_b}{q^2}T_3, \\ E &= C_{10}\frac{V}{m_B+m_\phi}, \\ F &= C_{10}(m_B+m_\phi)A_1, \\ G &= C_{10}\frac{A_2}{m_B+m_\phi}, \\ H &= 2C_{10}\frac{m_\phi}{q^2}(A_3-A_0).\end{aligned} \tag{18}$$

Here A_0, A_1, A_2, A_3, V, T_1, T_2 and T_3 are the relevant form factors.

The matrix element in (17) leads to the following differential decay rate [17]

$$\frac{\mathrm{d}\Gamma}{\mathrm{d}s} = \frac{\alpha^2 G_{\rm F}^2 m_B}{2^{12}\pi^5}|V_{tb}V_{ts}^*|^2\sqrt{\lambda_\phi}v\Delta_\phi, \tag{19}$$

where

$$\begin{aligned}\Delta_\phi = &\frac{8}{3}\lambda_\phi m_B^6 s((3-v^2)|A|^2 + 2v^2|E|^2) \\ &+ \frac{1}{r_\phi}\lambda_\phi m_B^4\Big[\frac{1}{3}\lambda_\phi m_B^2(3-v^2)|C|^2 + m_B^2 s^2(1-v^2)|H|^2 \\ &+ \frac{2}{3}[(3-v^2)W_\phi - 3s(1-v^2)]\mathrm{Re}[FG^*] \\ &- 2s(1-v^2)\mathrm{Re}[FH^*] \\ &+ 2m_B^2 s(1-r_\phi)(1-v^2)\mathrm{Re}[GH^*] \\ &+ \frac{2}{3}(3-v^2)W_\phi\mathrm{Re}[BC^*]\Big] \\ &+ \frac{1}{3r_\phi}m_B^2\Big[(\lambda_\phi + 12r_\phi s)(3-v^2)|B|^2 \\ &+ \lambda_\phi m_B^4[\lambda_\phi(3-v^2) - 3s(s-2r_\phi-2)(1-v^2)]|G|^2 \\ &+ (\lambda_\phi(3-v^2) + 24r_\phi s v^2)|F|^2\Big],\end{aligned} \tag{20}$$

where $s = q^2/m_B^2$, $r_\phi = m_\phi^2/m_B^2$, $v = (1-(4t^2/s))^{1/2}$, $t = m_l/m_B$, $\lambda_\phi = r_\phi^2 + (s-1)^2 - 2r_\phi(s+1)$ and $W_\phi = -1 + r_\phi + s$. Here, $z = \cos\theta$, where θ is the angle between the three-momentum of the ℓ^- lepton and that of the B_s-meson in the center of mass frame of the dileptons $\ell^+\ell^-$.

The $A_{\rm FB}$ is another observable that can give more precise information at the hadronic level. We write its definition as given by

$$A_{\rm FB}(s) = \frac{\int_0^1 \mathrm{d}z\frac{\mathrm{d}\Gamma}{\mathrm{d}z} - \int_{-1}^0 \mathrm{d}z\frac{\mathrm{d}\Gamma}{\mathrm{d}z}}{\int_0^1 \mathrm{d}z\frac{\mathrm{d}\Gamma}{\mathrm{d}z} + \int_{-1}^0 \mathrm{d}z\frac{\mathrm{d}\Gamma}{\mathrm{d}z}}, \tag{21}$$

where Γ is the total decay rate. The $A_{\rm FB}$ for the $B_s \to \phi\ell^+\ell^-$ decay is calculated to be

$$\begin{aligned}A_{\rm FB} = &\int \mathrm{d}s 8m_B^4\lambda_\phi v^2 s(\mathrm{Re}[BE^*] + \mathrm{Re}[AF^*]) \\ &\Big/ \int \mathrm{d}s\sqrt{\lambda_\phi}v\Delta_\phi.\end{aligned} \tag{22}$$

3 Numerical results and discussion

In this section we present the numerical analysis of the exclusive $B_s \to \phi\ell^+\ell^-$ decay in the 2HDMs. The input parameters we used in this analysis are as follows:

$$\begin{aligned}&m_{B_s} = 5.28\,\mathrm{GeV}, \quad m_b = 4.8\,\mathrm{GeV}, \\ &m_c = 1.4\,\mathrm{GeV}, \quad m_\mu = 0.105\,\mathrm{GeV}, \quad m_\tau = 1.77\,\mathrm{GeV}, \\ &m_\phi = 1.02\,\mathrm{GeV}, \quad m_{H^\pm} = 400\,\mathrm{GeV}, \quad |V_{tb}V_{ts}^*| = 0.04, \\ &\alpha^{-1} = 129, \quad G_{\rm F} = 1.17\times10^{-5}\,\mathrm{GeV}^{-2}, \\ &\tau_{B_s} = 1.54\times10^{-12}\,\mathrm{s}.\end{aligned} \tag{23}$$

The masses of the charged Higgs, $m_{H^\pm}$, the Yukawa couplings ($\xi_{ij}^{U,D}$) and the ratio of the vacuum expectation values of the two Higgs doublets, $\tan\beta$, remain as free parameters of the model. The restrictions on $m_{H^\pm}$, and $\tan\beta$ have been already discussed in Sect. 2. For Yukawa couplings, we use the restrictions coming from CLEO data [36],

$$\mathrm{BR}(B\to X_s\gamma) = (3.15\pm0.35\pm0.32)10^{-4}, \tag{24}$$

B^0–$\bar{B}^0$ mixing [33], the ρ parameter [30], and the neutron electric-dipole moment [37], which yields $\bar{\xi}_{N,ib}^D \sim 0$ and

Table 1. The values of the parameters in (26) for the various form factors of the transition $B \to \phi$ calculated in the light-cone QCD sum rule approach (QCDSR) [19] and using a constituent quark–meson model (CQM) [20]

	QCDSR			CQM		
	$F(0)$	a_F	b_F	$F(0)$	a_F	b_F
$A_1^{B\to\phi}$	0.30	0.87	−0.06	0.59	−0.11	0.49
$A_2^{B\to\phi}$	0.26	1.55	0.51	0.73	0.78	−0.52
$V^{B\to\phi}$	0.43	1.75	0.74	0.20	0.65	0.96
$T_1^{B\to\phi}$	0.35	1.82	0.83	0.21	0.78	0.07
$T_2^{B\to\phi}$	0.35	0.70	−0.32	0.21	0.85	12.9
$T_3^{B\to\phi}$	0.26	1.52	0.38	0.18	0.62	−0.88

$\bar{\xi}^D_{N,ij} \sim 0$, where the indices i, j denote d and s quarks, and $\bar{\xi}^U_{N,tc} << \bar{\xi}^U_{N,tt}$. Therefore, we take into account only the Yukawa couplings of the b and t quarks, $\bar{\xi}^U_{N,tt}$, $\bar{\xi}^D_{N,bb}$. There is also a restriction on the Wilson coefficient $C_7^{\rm eff}$ from the BR of $B \to X_s\gamma$ in (24) as follows [33]:

$$0.257 \leq |C_7^{\rm eff}| \leq 0.439. \tag{25}$$

In our numerical calculations for $B_s \to \phi\ell^+\ell^-$ decay, we use a three parameter fit of the light-cone QCD sum rule [19] which can be written in the following form:

$$F(q^2) = \frac{F(0)}{1 - a_F q^2/m_B^2 + b_F(q^2/m_B^2)^2}, \tag{26}$$

where the values of the parameters $F(0)$, a_F and b_F are given in Table 1. This table also contains the values of these parameters as calculated in the CQM [20], which we use to calculate the SM predictions for the BR in Table 2. The form factors A_0 and A_3 in (26) can be found from the following parameterization:

$$A_0 = A_3 - \frac{T_3 q^2}{m_\phi m_b},$$
$$A_3 = \frac{m_B + m_\phi}{2m_\phi} A_1 - \frac{m_B - m_\phi}{2m_\phi} A_2. \tag{27}$$

We note that there are five possible resonances in the $c\bar{c}$ system that can contribute to the decay under consideration and to calculate them, we need to divide the integration region for q^2 into three parts for $\ell = e, \mu$ so that we have $4m_\ell^2 \leq q^2 \leq (m_{\psi_1} - 0.02)^2$ and $(m_{\psi_1} + 0.02)^2 \leq q^2 \leq (m_{\psi_2} - 0.02)^2$ and $(m_{\psi_2} + 0.02)^2 \leq q^2 \leq (m_B - m_\phi)^2$, while for $\ell = \tau$ it takes the form given by $4m_\tau^2 \leq q^2 \leq (m_{\psi_2} - 0.02)^2$ and $(m_{\psi_2} + 0.02)^2 \leq q^2 \leq (m_B - m_\phi)^2$. Here, m_{ψ_1} and m_{ψ_2} are the masses of the first and the second resonances, respectively. The SM predictions for the integrated branching ratios for $\ell = e, \mu, \tau$ are presented in Table 2 for distinct q^2 regions and also the total contributions.

In the following, we give the results of our calculations on the dependences of the differential branching ratio ($\mathrm{dBR/d}q^2$) and $A_{\rm FB}(q^2)$ of the $B_s \to \phi\mu^+\mu^-$ decay on the four-momentum transfer q^2, and also dependences of BR and $A_{\rm FB}$ on the model parameters. The results are presented by a series of graphs, which are plotted for $\ell = \mu$ and for the case of the ratio $|r_{tb}| \equiv |\bar{\xi}^D_{N,tt}/\bar{\xi}^D_{N,bb}| < 1$. We do not present the results for the $r_{tb} > 1$ case, since BR for the $r_{tb} > 1$ case indicates one to two orders of magnitude enhancement with respect to the SM results, which seems to conflict with the experimental data given by the BELLE collaboration [39] for the inclusive $B \to X_s\ell^+\ell^-$ decays:

$$\mathrm{BR}(B \to X_s\ell^+\ell^-) = (7.1 \pm 1.6^{+1.4}_{-1.2}) \times 10^{-6}. \tag{28}$$

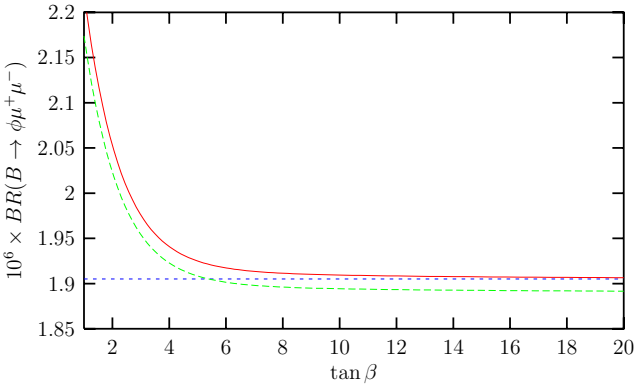

Fig. 1. The dependence of the BR of the $B_s \to \phi\mu^+\mu^-$ decay on $\tan\beta$. Here the solid (dashed) curve represents the model I (II) contribution, while the small dashed straight line is for the SM case

In Fig. 1, we plot the dependence of the BR of the $B_s \to \phi\mu^+\mu^-$ decay on $\tan\beta$ by taking $m_{H^\pm} = 400$ GeV. Here the solid (dashed) curve represents the model I (II) prediction for the BR and the small dashed straight line is for the SM result. We see that BR decreases with increasing values of $\tan\beta$. For $1 \lesssim \tan\beta \lesssim 4$, it is possible to enhance the BR $15(13)\% - 2(1.5)\%$ in model I (II) compared to its value in the SM. However the larger values of $\tan\beta$ have been favored by the recent experimental results [38]. We can therefore conclude that the charged Higgs boson contributions calculated in the context of the model I and II versions of the 2HDM are not very sizable, i.e., when $\tan\beta \gtrsim 5$ it almost coincides with the SM result in model I, while in model II, its value remains slightly below the SM one.

We have the following prescription for the graphs we give in between Figs. 2–6: the regions between the solid curves represent the $C_7^{\rm eff} > 0$ case, the regions between the dashed curves represent the $C_7^{\rm eff} < 0$ case, and the small dashed curves are for the SM predictions.

The dependence of the $\mathrm{dBR/d}q^2$ on q^2 is given in Fig. 2 in model III, including the long distance contributions. We see that $\mathrm{dBR/d}q^2$ almost coincides with the SM result for $C_7^{\rm eff} < 0$, while for the $C_7^{\rm eff} > 0$ cases it is considerably enhanced.

The dependence of the BR on one of the free parameters of model III, $\bar{\xi}^D_{N,bb}/m_b$ is shown in Fig. 3. It is seen from this figure that BR is not very much sensitive to $\bar{\xi}^D_{N,bb}/m_b$, especially for large values of this parameter. We

Table 2. The SM predictions for the integrated branching ratios for $\ell = e, \mu, \tau$ of the $B_s \to \phi\ell^+\ell^-$ decay for distinct q^2 regions and also the total contributions. Here, QCDSR (CQM) stands for the results calculated with the form factors of [19] ([20])

ℓ	Short distance contribution to the BR	$4m_l^2 \le q^2 \le (m_{\psi_1} - 0.02)^2$	$(m_{\psi_1} + 0.02)^2 \le q^2 \le (m_{\psi_2} - 0.02)^2$	$(m_{\psi_2} + 0.02)^2 \le q^2 \le (m_B - m_\phi)^2$	Short+Long distance contribution to the BR
e (QCDSR)	2.01×10^{-6}	1.50×10^{-6}	4.75×10^{-7}	3.70×10^{-7}	2.35×10^{-6}
(CQM)	1.87×10^{-6}	1.59×10^{-6}	3.10×10^{-7}	1.80×10^{-7}	2.08×10^{-6}
μ (QCDSR)	1.65×10^{-6}	1.00×10^{-6}	4.74×10^{-7}	3.69×10^{-7}	1.91×10^{-6}
(CQM)	1.25×10^{-6}	0.96×10^{-7}	3.07×10^{-7}	1.08×10^{-7}	1.45×10^{-6}
τ (QCDSR)	1.38×10^{-7}	3.01×10^{-8}	9.47×10^{-8}		1.25×10^{-7}
(CQM)	2.28×10^{-7}	3.42×10^{-8}	1.75×10^{-7}		2.09×10^{-7}

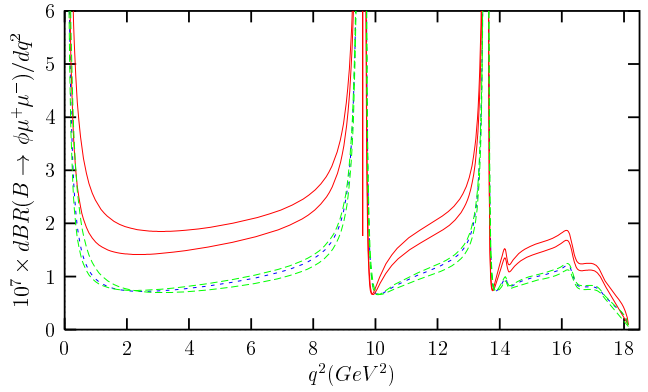

Fig. 2. The dependence of $\mathrm{dBR/d}q^2$ on q^2. Here the region between the solid curves represents $\mathrm{dBR/d}q^2$ for $C_7^{\rm eff} > 0$, while the one between the dashed curves is for $C_7^{\rm eff} < 0$. The SM prediction is represented by the small dashed curve. Here we take $\bar{\xi}^D_{N,bb} = 40 m_b$

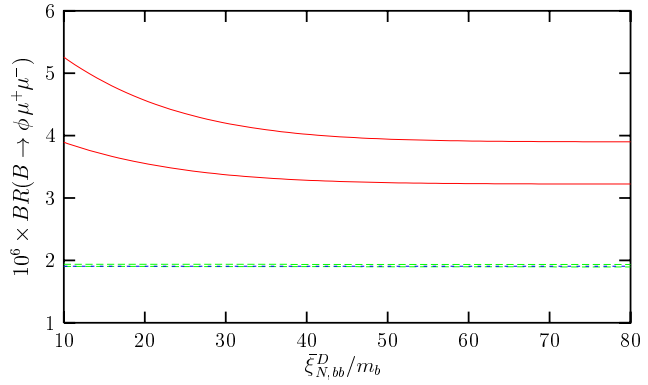

Fig. 3. The dependence of the BR on $\bar{\xi}^D_{N,bb}/m_b$. Here the BR is restricted to the region between the solid (dashed) curves for $C_7^{\rm eff} > 0$ ($C_7^{\rm eff} < 0$). The small dashed straight line represents the SM prediction

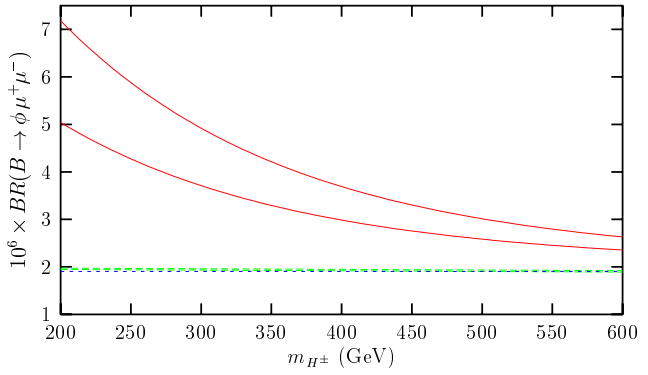

Fig. 4. The dependence of the BR on $m_{H^\pm}$ for $\bar{\xi}^D_{N,bb} = 40 m_b$. Here the BR is restricted to the region between the solid (dashed) curves for $C_7^{\rm eff} > 0$ ($C_7^{\rm eff} < 0$). The small dashed straight line represents the SM prediction

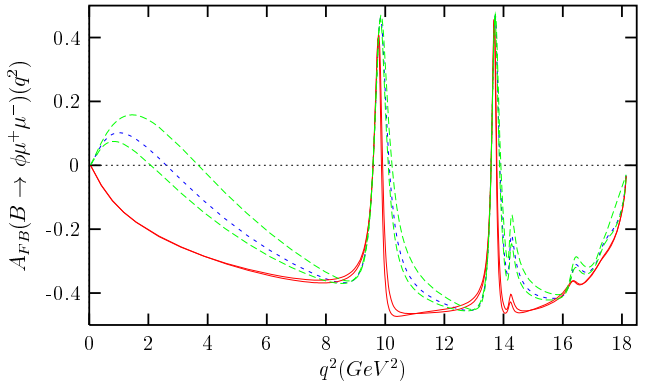

Fig. 5. The dependence of $A_{\rm FB}(q^2)$ on q^2. Here the region between the solid curves represents the $A_{\rm FB}(q^2)$ for $C_7^{\rm eff} > 0$, while the one between the dashed curves is for $A_{\rm FB}(q^2)$ for $C_7^{\rm eff} < 0$. The SM prediction is represented by the small dashed curve. Here we take $\bar{\xi}^D_{N,bb} = 40 m_b$

note that the SM and model III average results for BR when $C_7^{\rm eff} > 0$ ($C_7^{\rm eff} < 0$) are 1.91×10^{-6} and 4.00×10^{-6} (1.91×10^{-6}).

The dependence of the BR on the charged Higgs mass $m_{H^\pm}$ is presented in Fig. 4. The BR decreases as $m_{H^\pm}$ increases, except for the $C_7^{\rm eff} < 0$ case, which is insensitive to $m_{H^\pm}$ and very close to the SM prediction in magnitude.

We present the dependence of the $A_{\rm FB}(q^2)$ on q^2 for the $B_s \to \phi\mu^+\mu^-$ decay in Fig. 5. Here, the $A_{\rm FB}(q^2)$ is enhanced for $C_7^{\rm eff} > 0$ while it almost coincides with the SM prediction for $C_7^{\rm eff} > 0$.

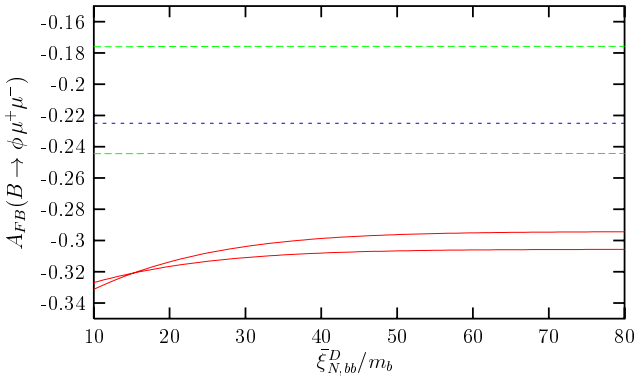

Fig. 6. The dependence of $A_{\rm FB}$ on $\bar{\xi}^D_{N,bb}$. Here $A_{\rm FB}$ is restricted to the region between the solid (dashed) curves for $C_7^{\rm eff} > 0$ ($C_7^{\rm eff} < 0$). The small dashed straight line represents the SM prediction

In Fig. 6, the dependence of $A_{\rm FB}$ on $\bar{\xi}^D_{N,bb}/m_b$ is represented. We observe that $A_{\rm FB}$ is not very sensitive to $\bar{\xi}^D_{N,bb}/m_b$, especially for large values of this parameter. The SM and model III average results for $A_{\rm FB}$ when $C_7^{\rm eff} > 0$ ($C_7^{\rm eff} < 0$) are -0.23 and -0.31 (-0.21).

In conclusion, we have investigated the physical observables BR and $A_{\rm FB}$ related to the exclusive $B_s \to \phi\ell^+\ell^-$ decay in the model I, II and III versions of the 2HDM. We have found that these observables are highly sensitive to new physics and hence provide a powerful probe of the SM.

References

1. J.L. Hewet, in Proceedings of the 21st Annual SLAC Summer Institute, edited by L. De Porcel, C. Dunwoode, SLAC-PUB-6521 (1994)
2. T. Affolder et al., CDF Collaboration, Phys. Rev. Lett. **83**, 3378 (1999)
3. K. Abe et al., Belle Collaboration, Phys. Rev. Lett. **88**, 021801 (2002)
4. N.G. Deshpande, J. Trampetić, Phys. Rev. Lett. **60**, 2583 (1988)
5. D.S. Du, C. Liu, Phys. Lett. B **317**, 179 (1993)
6. G. Burdman, Phys. Rev. D **52**, 6400 (1995); W. Roberts, Phys. Rev. D **54**, 863 (1996)
7. D.S. Liu, Phys. Rev. D **52**, 5056 (1995)
8. C. Greub, A. Ioannissian, D. Wyler, Phys. Lett. B **346**, 149 (1995)
9. C.Q. Geng, C.P Kao, Phys. Rev. D **54**, 5636 (1996)
10. D. Melikhov, N. Nikitin, S. Simula, Phys. Lett. B **442**, 381 (1998)
11. T.M. Aliev, M. Savci, A. Özpineci, H. Koru, J. Phys. G **24**, 49 (1998)
12. A. Ali, P. Ball, L.T. Handoko, G. Hiller, Phys. Rev. D **61**, 074024 (2000)
13. F. Krüger, J.C. Romão, Phys. Rev. D **62**, 034020 (2000)
14. T.M. Aliev, C.S. Kim, Y.G. Kim, Phys. Rev. D **62**, 014026 (2000)
15. T.M. Aliev, M. Savci, Phys. Lett. B **481**, 275 (2000)
16. T.M. Aliev, A. Özpineci, M. Savci, Phys. Lett. B **511**, 49 (2001)
17. T.M. Aliev, M.K. Cakmak, M. Savci, Nucl. Phys. B **607**, 305 (2001)
18. G. Erkol, G. Turan, Nucl. Phys. B **635**, 296 (2002)
19. P. Ball, J. High Energy Physics **09**, 005 (1998); P. Ball, V.M. Braun, Phys. Rev. D **58**, 094016 (1998)
20. A. Deandrea, A.D. Polosa, Phys. Rev. D **64**, 074012 (2001)
21. F. Krüger, L.M. Sehgal, Phys. Rev. D **56**, 5452 (1997); D **60**, 099905 (1999) (E)
22. F. Krüger, L.M. Sehgal, Phys. Rev. D **55**, 2799 (1997)
23. S. Bertolini, F. Borzumati, A. Masiero, G. Ridolfi, Nucl. Phys. B **353**, 591 (1991)
24. T.M. Aliev, M. Savci, Phys. Rev. D **60**, 14005 (1999)
25. E.O. Iltan, Int. J. Mod. Phys. A **14**, 4365 (1999)
26. G. Erkol, G. Turan, J. High Energy Phys. **02**, 015 (2002)
27. S. Glashow, S. Weinberg, Phys. Rev. D **15**, 1958 (1977)
28. D. Buskulic et al., ALEPH Collaboration, Phys. Lett. B **343**, 444 (1995); J. Kalinowski, Phys. Lett. B **245**, 201 (1990); A.K. Grant, Phys. Rev. D **51**, 207 (1995)
29. T.P. Cheng, M. Sher, Phys. Rev D **35**, 3484 (1987); D **44**, 1461 (1991); W.S. Hou, Phys. Lett. B **296**, 179 (1992); A. Antaramian, L. Hall, A. Rasin, Phys. Rev. Lett **69**, 1871 (1992); L. Hall, S. Weinberg, Phys. Rev D **48**, 979 (1993); M.J. Savage, Phys. Lett. B **266**, 135 (1991)
30. D. Atwood, L. Reina, A. Soni, Phys. Rev. D **55**, 3156 (1997)
31. B. Grinstein, R. Springer, M.B. Wise, Nucl. Phys. B **339**, 269 (1990); R. Grigjanis, P.J. O'Donnell, M. Sutherland, H. Navelet, Phys. Lett. B **213**, 355 (1988); Phys. Lett. B **286**, 413 (1992); G. Cella, G. Curci, G. Ricciardi, A. Viceré, Phys. Lett. B **325**, 227 (1994); Nucl. Phys. B **431**, 417 (1994)
32. M. Misiak, Nucl. Phys. B **393**, 23 (1993); B **439**, 461 (1995) (E)
33. T.M. Aliev, E.O. Iltan, J. Phys. G Nucl. Part. Phys. **25**, 989 (1999)
34. A.J. Buras, M. Münz, Phys. Rev. D **52**, 186 (1995)
35. A. Ali, T. Mannel, T. Morozumi, Phys. Lett. B **273**, 505 (1991)
36. M.S. Alam, et al., CLEO Collaboration, in ICHEP98 Conference 1998; R. Barate et al., ALEPH Collaboration, Phys. Lett. B **429**, 169 (1998)
37. D. Bowser-Chao, K. Cheung, W-Y. Keung, Phys. Rev. D **59**, 115006 (1999)
38. A. Heister et al., ALEPH Collaboration, CERN-EP/2001-095; L3 Collaboration, Phys. Lett. B **503**, 21 (2001)
39. J. Kaneko, Study of the flavor changing neutral current decay $B \to X_s\ell^+\ell^-$ (talk given at the DPF-2002 Conference), http://www.dpf2002.org